Contrails

WADD TECHNICAL REPORT 61-72
VOLUME V

RESEARCH AND DEVELOPMENT ON ADVANCED GRAPHITE MATERIALS

VOL V. – ANALYSIS OF CREEP AND RECOVERY CURVES FOR ATJ GRAPHITE

E. J. SELDIN
R. N. DRAPER

RESEARCH LABORATORY
NATIONAL CARBON COMPANY
DIVISION OF UNION CARBIDE CORPORATION

SEPTEMBER 1961

DIRECTORATE OF MATERIALS AND PROCESSES
CONTRACT No. AF 33(616)-6915
PROJECT Nos. 7350, 7381 and 7-817

USAF AERONAUTICAL SYSTEMS DIVISION
AIR FORCE SYSTEMS COMMAND
UNITED STATES AIR FORCE
WRIGHT-PATTERSON AIR FORCE BASE, OHIO

800 - December 1961 - 15-609 & 610

Approved for Public Release

Contrails

FOREWORD

This work was conducted by the National Carbon Company, Division of Union Carbide Corporation under USAF Contract AF 33(616)-6915. This contract was initiated under WADD Materials Central Project No. 7350 "Refractory Inorganic Non-Metallic Materials," Task No. 73503, "Graphite Materials Development"; Project No. 7381 "Materials Application," Task No. 73811 "Materials Preproduction Process Development"; and AMC Aeronautical Systems Center, Directorate of Advanced Systems and Production, Project No. 7-817, "Process Development for Graphite Materials." The work was administered under the combined direction of the Materials Central, Directorate of Advanced Systems Technology, Wright Air Development Division, with Captain R. H. Wilson and Mr. C.W. Douglass acting as project engineers and the Manufacturing and Materials Technology Division, Directorate of Advanced Systems and Production, AMC Aeronautical Systems Center with Major C. P. Fritsch acting as project engineer.

Work under this contract has been in progress since May 1, 1960. The work covered in this report was conducted at the Research Laboratory of the National Carbon Company located at Parma 30, Ohio, under the direction of J. C. Bowman, Director of Research, and W. P. Eatherly, Assistant Director of Research.

This is the fifth of a series of volumes of WADD Technical Report 61-72 prepared to describe various phases of the work. The preceding volumes of this series are:

Volume I - Observations by Electron Microscopy of Dislocations in Graphite, by Richard Sprague.

Volume II - Applications of Anisotropic Elastic Continuum Theory to Dislocations in Graphite, by G. B. Spence.

Volume III - Decoration of Dislocations and Low Angle Grain Boundaries in Graphite Single Crystals, by Roger Bacon and Richard Sprague.

Volume IV - Adaptation of Radiographic Principles to the Quality Control of Graphite, by R. W. Wallouch.

Approved for Public Release

Contrails

ABSTRACT

Flexural creep tests have been made on specimens of ATJ graphite at temperatures ranging from 2300°C to 3000°C. The creep curves have been fitted by graphical and analytical means to four equations. Fairly good fits have been obtained with all of the equations which were used. Attempts were made to determine the stress and temperature dependence of several of the parameters in the equations.

Of the four equations which were used, one could be related to simple rheological models having some physical significance. A model was found useful not only in describing the creep curves, but also in describing the recovery after creep and relating the behavior in recovery to the behavior during creep. Generally good agreement was found between the qualitative predictions of the models and the observed behavior. Using a model, an activation energy for the steady state creep rate was determined to lie between 70 and 76 kcal/mole. Some deviations were detected between the actual behavior of the material and that predicted by the simple models which suggest some modifications that may be made to obtain a better model. The value of a model is discussed, and several additional experiments are suggested to supplement the information given by creep experiments.

PUBLICATION REVIEW

This report has been reviewed and is approved.

FOR THE COMMANDER:

W. G. RAMKE
Chief, Ceramics and Graphite Branch
Metals and Ceramics Laboratory
Directorate of Materials & Processes

Approved for Public Release

Contrails

TABLE OF CONTENTS

Approved for Public Release

Contrails

LIST OF FIGURES

Approved for Public Release

Contrails

LIST OF TABLES

Approved for Public Release

Contrails

I. INTRODUCTION

In recent years, several authors[1, 2] have proposed and tested a number of equations to describe and characterize the high temperature creep of carbons and graphite. These equations, which give the deformation X in time t, are as follows:

$$X = A + Bt + C \log t \quad (1)$$

$$X = D + Et + F\,(1-e^{-\alpha t}) \quad (2)$$

$$X = G + Ht^{\beta} \quad (3)$$

$$X = Kt^{\gamma} \quad (4)$$

These equations, or parts of some of them, have been used to describe creep in metals and other materials by many authors for many years, so that all have some basis either in theory or in practical use. The terms linear in time in equations (1) and (2) describe the steady state creep common to most materials. The logarithmic function of time in equation (1) can be found in the literature on the exhaustion theory of transient creep,[3] but no theoretical justification for this type of behavior for creep in carbon has as yet been advanced. Equation (2) is a well known equation for the creep of viscoelastic materials, and can be related to some simple rheological models. The power laws in equations (3) and (4) are empirical equations. Equation (3), with $\beta = 1/3$, is Andrade's law for creep, which has been found to hold true for many metals.

In the literature on graphite, equation (1) was proposed by Davidson and Losty,[1] who used it to describe the creep of graphite cantilevers and springs in the temperature range of 1000°C to 2000°C. They found the parameters B and C to be Arrhenius functions of the temperature, i.e., $B \sim \exp(-U/RT)$, with activation energies U ranging from 20 to 50 kcal/mole. The equation was also used by Martens,[2] et al, for the creep of graphite in tension in the temperature range of 2440°C to 2900°C. The latter authors also found B and C to be Arrhenius functions of the temperature with activation energies of 106 and 112 kcal/mole, respectively. They also fitted their creep data to equations (2) and (3) and found that the creep could be fitted equally as well by any of the first three equations. In using equation (2), Martens[2] and coauthors found E and $1/\alpha$ to be Arrhenius functions, with activation energies of 178 and 148 kcal/mole, respectively. In equation (3), they found that H could also be approximated by an Arrhenius function with an activation energy of 98 kcal/mole and the exponent β varied considerably with each sample, but had an average value of 0.49.

Manuscript released by the authors May 1961 for publication as a WADD Technical Report.

Approved for Public Release

Contrails

This paper presents the results of an attempt to analyze the creep data for ATJ graphite using the four preceding equations. The creep test was one of simple flexure. The principal advantages of a flexural test are to be found in the relative simplicity of the experimental apparatus and procedure and the ease in specimen preparation. One serious disadvantage of a flexure experiment is that the stress is concentrated in a very small region of the specimen and the creep behavior will be greatly influenced by the presence of small flaws or density variations within the small region of high stress concentration. This leads to considerably more scatter in the data than one would anticipate in a tensile test where the influence of flaws and inhomogeneities in the sample, provided they are small compared to the cross section of the sample, would tend to average out over the length of the sample. Another disadvantage of a flexure test is that the stress distribution within the specimen changes in a complex manner as the specimen is deformed, making it very difficult to relate the deformation to strain. However, by conducting a sufficiently large number of tests in which the temperature and stress were varied over fairly wide ranges, a fairly clear pattern of behavior could be detected.

The experimentally obtained creep curves for individual specimens have been fitted to each of the four equations by a combination of graphical analysis and the method of least squares analysis. The parameters in each of the four equations have been determined, and the attempt has been made to find correlations between the parameters of the equations and the stress and temperature. The usual stress dependence which was sought was either a power law or an exponential function, and those parameters which are coefficients of terms containing the time were usually tested to see whether they were Arrhenius functions of the temperature. It has been found that each of the equations is capable of fitting any of the individual creep curves, and no one equation stands out as being better than all the rest as far as its ability to fit the data is concerned. In no one equation can all of the parameters be expressed as simple functions of the stress and temperature.

Since there is at the present time no theoretical basis for an equation for describing creep in carbons in terms of a model involving atomic mechanisms, the four equations presented here represent the best guesses for a functional dependence of the deformation on the time that have been made to date. But the choice of one equation in preference to others is largely a matter of individual taste. The authors have found that equation (2), which can be related to some simple rheological models, is useful because carbons do behave at high temperature very much like viscoelastic materials. The models on which the equation is based were found to be useful in describing and interpreting in qualitative terms not only the creep, but the recovery after creep. Deviations were found between the actual stress and temperature dependence of the parameters and those assumed for the simple components of the model. While the models and the equation itself do have several limitations, and these limitations will be discussed, they are of value in characterizing the phenomenological aspects of the creep and may prove to be useful as a guide toward an explanation of the creep in terms of atomic mechanisms, which should be the ultimate goal of any investigation of creep.

Approved for Public Release

Contrails

2. EXPERIMENTAL PROCEDURE AND DATA

The creep specimens were 3/32 x 3/8 x 1-3/4-inch in size, and were all cut from a single large piece of ATJ graphite. The specimens were all cut in such a manner that the direction of applied molding pressure was perpendicular to the broad face of the specimens so that the grain orientation was the same in each specimen.

The creep tests were performed in a 4-inch diameter horizontal, resistance-heated graphite tube furnace in an inert atmosphere of argon. The creep fixture and other parts of the apparatus within the furnace were made of graphite. The specimen was held in a vertical position, and the distance between the specimen supports was 1.5 inches. The load was applied against the broad face of the specimen by means of a knife-edge which was placed midway between the supports. The specimen was brought to temperature, and a constant force was applied to the knife-edge through a graphite load transmission rod which ran from the knife-edge to the outside of the furnace. The constant load was attained by means of a dead weight, pulley, and lever arrangement. The deformation as a function of time was observed by plotting on a Varian recorder the output of a linear variable differential transformer which followed the motion of the load transmission rod outside the furnace. The creep tests were run at temperatures of 2300, 2400, 2600, 2800, 2900, and 3000°C, with applied loads of 250, 500, 1000, 1500, 2000, and 2500 grams. The experimentally obtained creep curves are grouped according to temperature in Figures 1 through 6. The creep tests were all run for two hours with a load of 2500 g, except for the test at 3000°C where the run was terminated earlier because the deformation was approaching the maximum deformation which could be measured with the apparatus. In all cases, when the load was removed at the end of the two-hour run, there was an instantaneous elastic recovery, followed by a gradually decreasing rate of recovery. Though the recovery parts of the curves are not shown in the figures, they were observed for about 20 minutes. Mention is made in Section 4 of this paper of some of the features of these recovery curves and of some other experiments in which recovery curves were more closely examined.

Approved for Public Release

Contrails

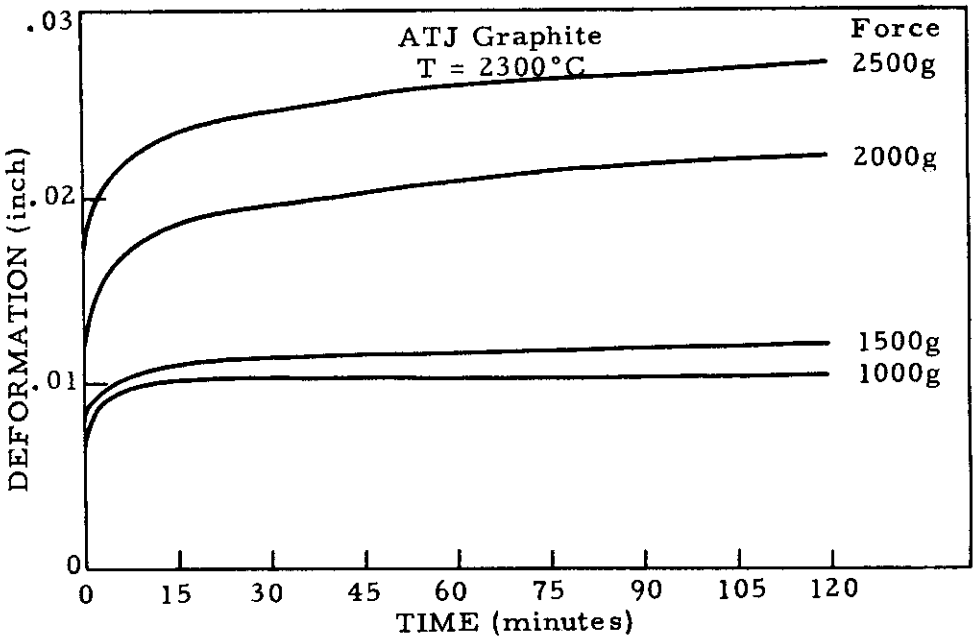

N-1110

Figure 1. - Creep of ATJ graphite at 2300°C.

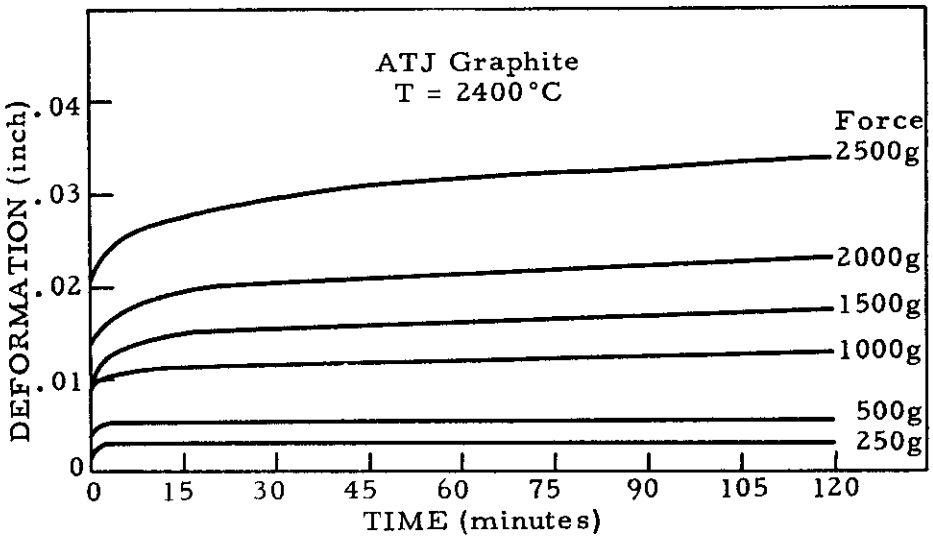

N-1111

Figure 2. - Creep of ATJ graphite at 2400°C.

Approved for Public Release

Contrails

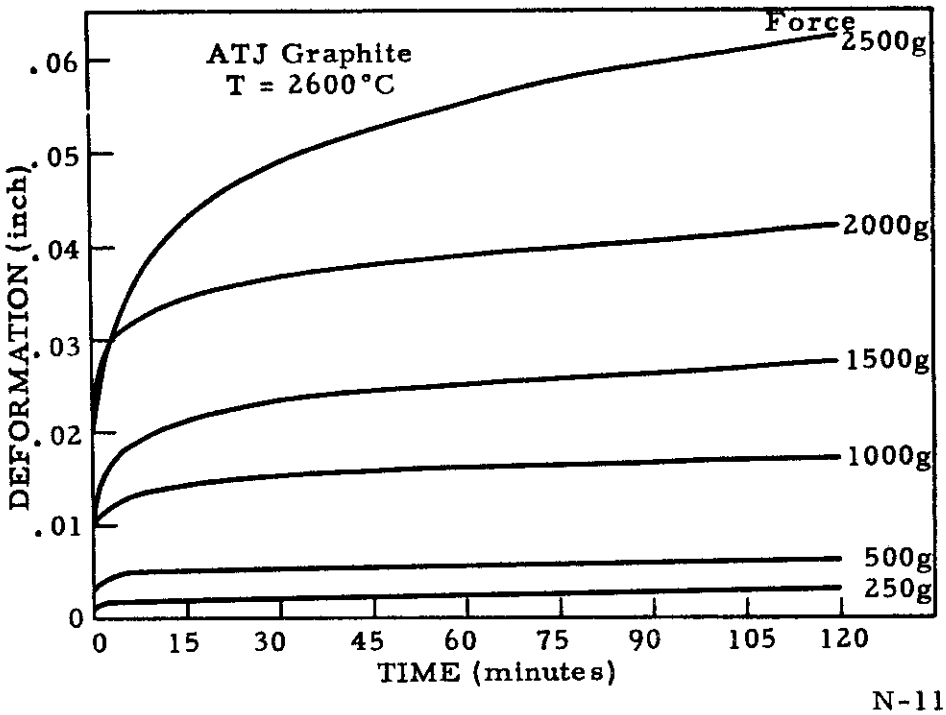

Figure 3. - Creep of ATJ graphite at 2600°C.

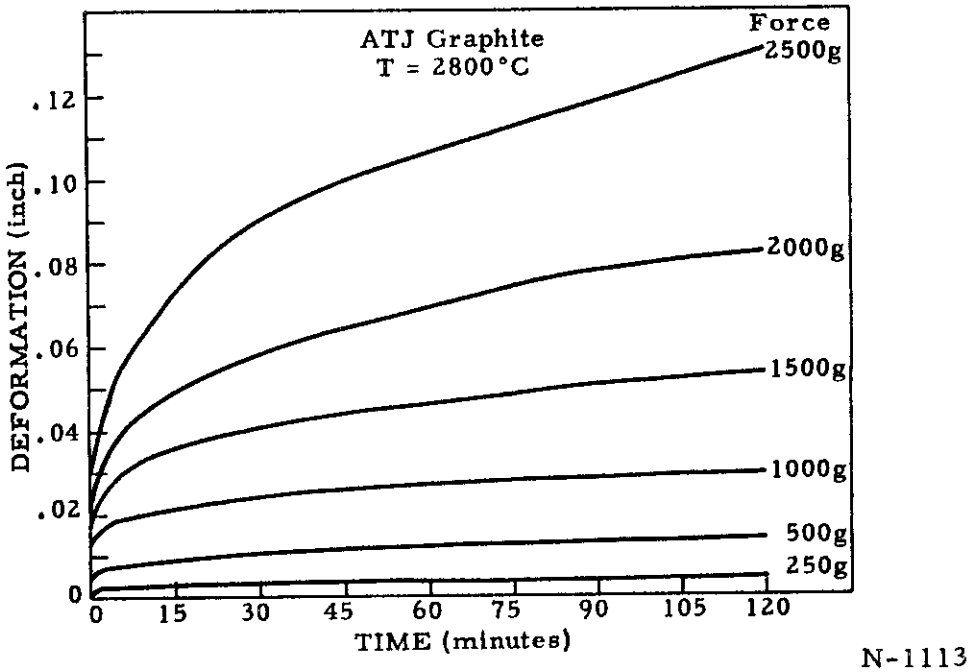

Figure 4. - Creep of ATJ graphite at 2800°C

Approved for Public Release

Contrails

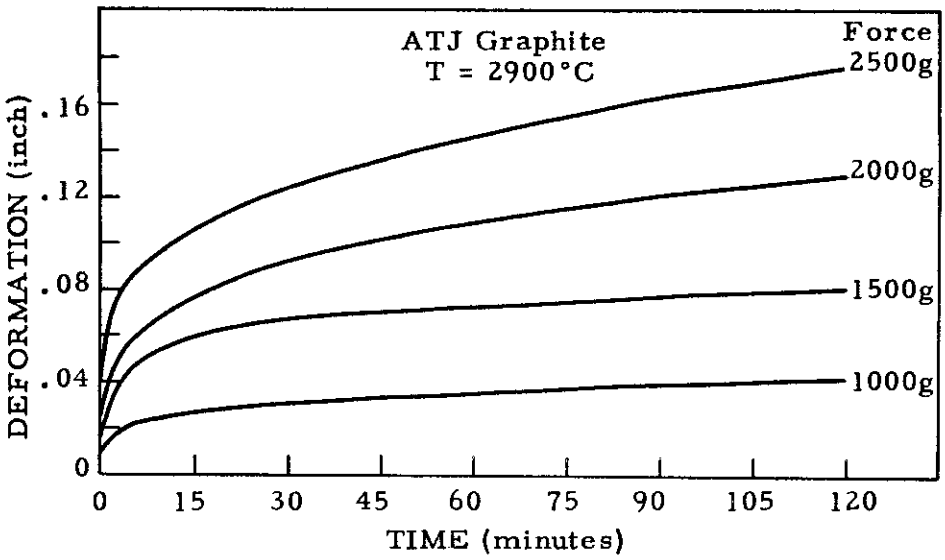

N-1114

Figure 5. - Creep of ATJ graphite at 2900°C.

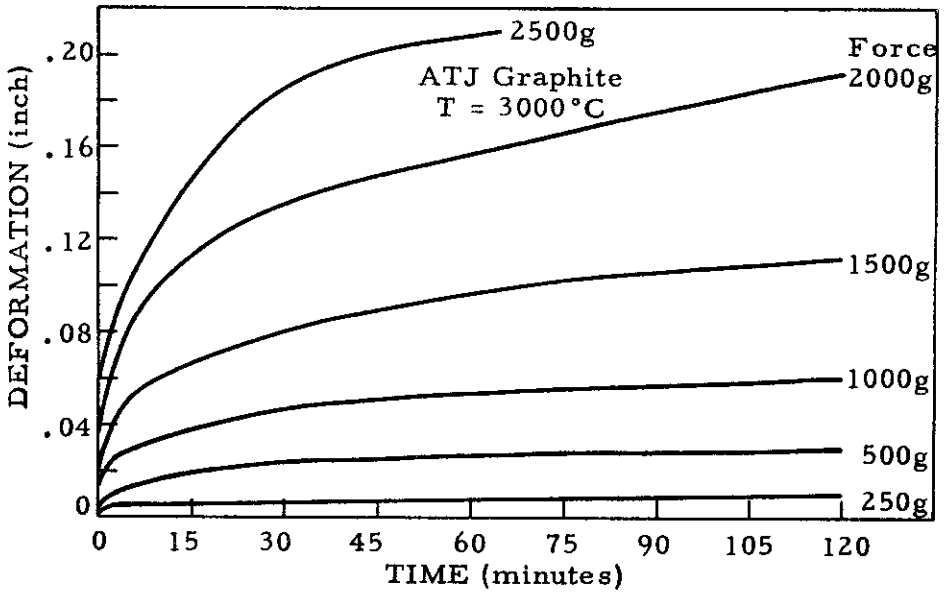

N-1115

Figure 6. - Creep of ATJ graphite at 3000°C.

Approved for Public Release

Contrails

3. CREEP ANALYSIS

The data from each of the experimentally obtained creep curves were tabulated at six-minute intervals, and each curve was fitted to each of the four equations presented in the "Introduction." Some of the parameters in the equations were determined from the curves by simple graphical analysis, and several were determined by the method of least squares analysis. Each equation will be discussed separately. Each equation was judged for goodness of fit, and the dependence of the parameters on temperature and stress was investigated. In the discussions that follow, the letter "X" will refer to the deformation of the sample as measured in inches, "P" to the applied load as measured in grams, "T" to the temperature, and "t" to the time as measured in minutes.

3.1 Equation (1) : $X = A + Bt + C \log t$

In the work of Davidson and Losty,[1] and of Martens,[2] et al, the parameters in equation (1) were obtained from a graphical analysis of the equation. To make the equation dimensionally correct, we should rewrite it as

$$X = A + Bt + C \log \frac{t}{t_0} \quad . \tag{1a}$$

For purposes of convenience, the time t was taken in minutes, and $t_0 = 1$. Equation (1) was rewritten by the above authors as

$$\frac{X-A}{t} = B + C \frac{\log t}{t} \quad , \tag{1b}$$

and $\frac{X-A}{t}$ was plotted against $\frac{\log t}{t}$. Since the data indicated that C is the dominant term and that Bt at t = 1 is much smaller than A, the value of A was taken directly from the creep curve as the value of X at t = 1. The data then were fitted to a straight line whose slope gave the value of C and whose intercept on the $\frac{X-A}{t}$ axis (as t becomes infinitely large) gave the value of B.

The function $\frac{\log t}{t}$ is a double valued function of the time with a maximum of 0.16 at t = e. In applying a least squares program to the data, equal intervals of $\frac{\log t}{t}$ were taken. (See Appendix I for the least squares program.) Intervals of $\frac{\log t}{t}$ of magnitude 0.0025 were chosen in the range 0.0200 to 0.500, which corresponds to values of t from 100 minutes to 29.3 minutes. As a result, the data were fitted to the equation in this interval of time. This procedure gave the

Approved for Public Release

Contrails

best straight line fit on the plot of $\frac{X-A}{t}$ vs $\frac{\log t}{t}$, but it weighted most heavily the values of the deformation at the lower times. In our analysis, the value of A was also taken directly from the creep curves as the value of X at t = 1, and the values of B and C were determined from the least squares analysis. From the values of A, B, and C which were thus determined, values of X could be calculated and compared with observed values.

Although no means of quantitatively evaluating goodness of fit has been attempted, it must be said that equation (1) fits the data very well. Figure 7 shows

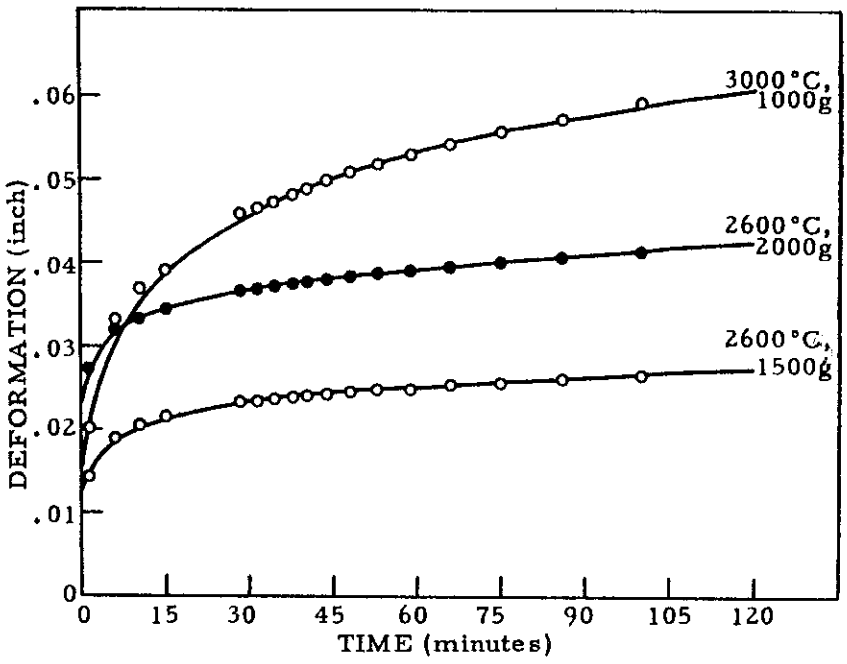

N-1116

Figure 7. - Fitting creep curves to equation (1); solid line-observed, circles-predicted by equation (1).

the fits which were obtained with three of the creep curves. In general, the best fit was found to be in the range t = 29.3 to t = 100 minutes, with the predicted values of X for shorter times tending to be a little greater than the observed values. Though none of our creep tests lasted longer than two hours, the data of Martens, [2] et al, indicate that good fits can be obtained for the first two hours' data, but that deviations from the predicted behavior as determined by equation (1) in the first two hours become larger as the time increases from two to four hours.

The values of the parameters obtained from fitting each of the creep curves to equation (1) are given in Table 1. One difficulty encountered with equation (1) was that of relating the parameters A, B, and C to P and T. Rather than present the considerable number of linear and logarithmic plots which were made to find some correlation between the parameters and the stress and temperature, only the conclusions drawn from inspection of these plots will be discussed.

Approved for Public Release

Table 1. - Parameter values obtained by fitting the creep curves to equations (1), (3), and (4).

Temperature °C	Force Grams	(1) $X = A + Bt + C \log t$			(3) $X = G + Ht^{\beta}$			(4) $X = Kt^{\gamma}$	
		$A \times 10^4$ Inch	$B \times 10^4$ Inch	$C \times 10^4$ Inch	$G \times 10^4$ Inch	$H \times 10^4$ Inch	β	$K \times 10^4$ Inch	γ
2300	1000	85	-.024	9.29	72	13.7	.202	80.6	.0607
	1500	90	-.024	15.3	72	24.2	.147	92.5	.0556
	2000	135	.014	40.2	112	42.3	.198	143	.0905
	2500	186	.039	39.8	168	39.9	.200	195	.0691
2400	250	19	.01	6.1	17	6.5	.173	22.3	.0742
	500	50	-.05	5.7	43	14	0	57	0
	1000	95	-.018	15.0	79	23.8	.136	99.6	.0465
	1500	109	-.09	33.2	86	42.5	.143	124	.0669
	2000	146	-.01	39.4	112	47.9	.188	149	.0898
	2500	201	.34	42.6	164	44.0	.271	181	.121
2600	250	12	.04	5.9	9	4.59	.301	11.3	.191
	500	36	.06	7.80	27	7.39	.313	28.4	.156
	1000	111	.08	25.5	85	34.9	.190	112	.0887
	1500	144	0	60.0	103	70.9	.179	163	.105
	2000	272	.254	58.4	218	67.0	.231	258	.101
	2500	254	.65	146	189	112	.287	259	.185
2800	250	18	.16	7.26	12	5.05	.425	12.1	.297
	500	61	.39	21.4	44	17.6	.367	47.7	.232
	1000	153	.34	53.2	115	48.9	.280	141	.159
	1500	216	.99	104	155	78.3	.351	180	.231
	2000	287	2.20	154	196	101	.389	224	.277
	2500	364	2.50	311	248	219	.321	392	.244
2900	1000	150	.60	93.8	99	75.0	.297	148	.212
	1500	294	-.09	244	170	247	.196	400	.149
	2000	393	2.2	312	274	210	.329	398	.244
	2500	661	2.9	315	356	273	.341	510	.257
3000	250	36	.16	21.9	30	13.7	.339	35	.217
	500	74	.38	93.6	46	68.1	.284	102	.233
	1000	199	.62	165	123	135	.270	229	.205
	1500	337	2.02	279	202	205	.319	344	.250
	2000	527	2.20	519	304	389	.290	609	.233
	2500	715	12.1	490	472	532	.473	906	.207

Approved for Public Release

Contrails

The parameter A appears to be roughly proportional to P^n with $n \approx 1.2$. If one sets $A = KP^{1.2}$ and evaluates K at each T and P, it is found that K increases almost linearly with the temperature. It is also possible, on a plot of A vs P to roughly fit the points by straight lines of the type $A = K'(P - P_0)$, where P_0 is an intercept value of about 150 g. This value of P_0 may correspond to a frictional resistance in the apparatus, though its value appears to be too high for friction. In the authors' opinion, neither the fit of the points to the power law or to the straight line is good enough to offer conclusive evidence for either relationship.

Another difficulty with equation (1) lies in the behavior of the parameter B. Examination of the values of B in Table 1 reveals that for low temperatures and loads, the value of B is sometimes negative. This occurs when the slope of the creep curve approaches zero. Since the log t term always has a positive slope and also dominates the equation, the B term must become negative. Furthermore, the behavior of B as a function of P tended to be considerably erratic.

The parameter C was found to be roughly proportional to P^n with $n = 1.4$. Figure 8 is a plot of log C vs 1/T, in which it appears that C can also be represented as an Arrhenius function, with an activation energy of about 78 kcal/mole. There is, however, a considerable amount of scatter of the points about the straight lines. It can be seen that we do not find that both B and C are Arrhenius functions of the temperature as did Davidson and Losty and Martens, et al.

3.2 Equation (3): $X = G + Ht^{\beta}$; and Equation (4): $X = Kt^{\gamma}$

In evaluating the parameters in equation (3), the value of G was read directly off the original creep data as the value of the "instantaneous elastic deformation." Since the initial deformation as observed on the recorder is actually not instantaneous, but occurs rather at a very rapid rate, it was difficult to get a very precise reading in many cases of the value of G. The values of G which were used were actually the values of the deformation within about the first five seconds after the load was applied, where the creep rate had definitely decreased from its initial very rapid rate. Using these values of G, the parameters H and B were evaluated by the least squares program given in Appendix II. The values of the parameters which were thus obtained are given in Table 1. The least squares program which was used for equation (4), which is a simple power law, is also given in Appendix II, and the values of the parameters K and γ are also given in Table 1.

Both of the power laws gave surprisingly good fits. Figure 9 shows the fits which were obtained with both of the above equations for the same three creep curves which are shown in Figure 7. For equation (3), the best fitting region was from 32 to 100 minutes, where the actual fitting was done. Generally, the values of X on the fitted curve were greater than the observed values for times less than about 15 minutes. The same situation appeared to hold for equation (4).

The parameter G showed an interesting relationship with both the stress and the temperature. It is identically equal to the parameter D in equation (2). It corresponds to an instantaneous elastic deformation, and will be discussed more fully in the next section where a mechanical model is considered.

Approved for Public Release

Contrails

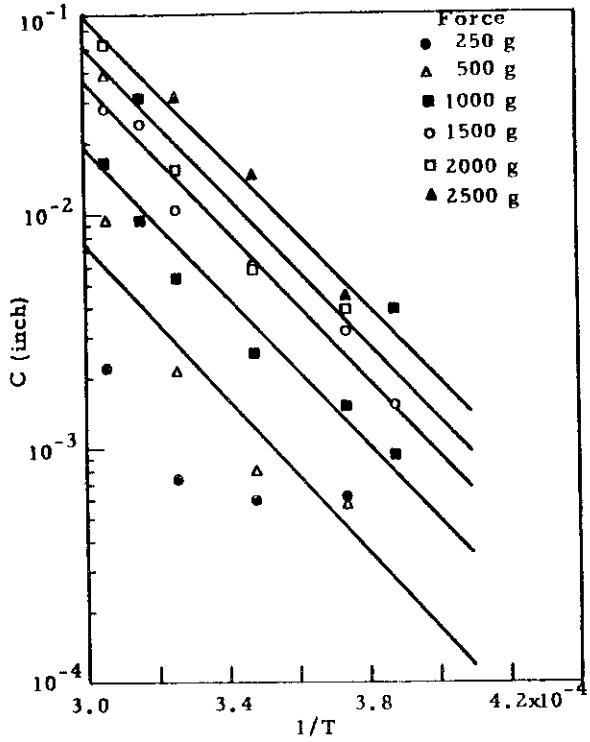

N-1117

Figure 8. - Plot of log C vs 1/T.

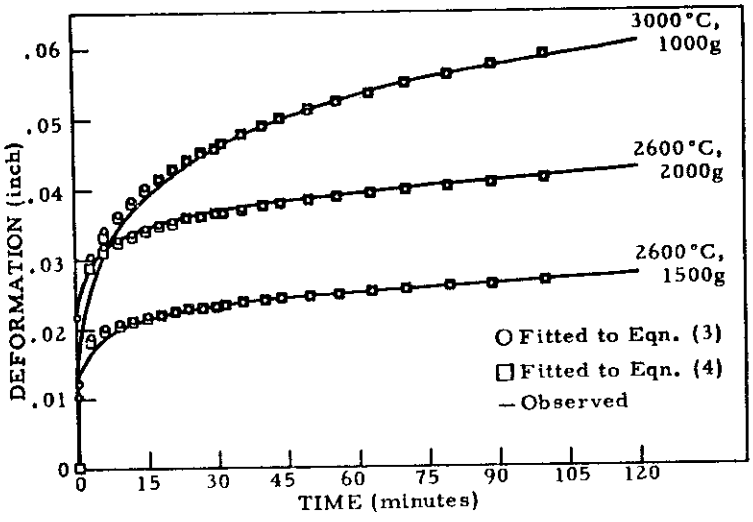

N-1118

Figure 9. - Fitting creep curves to equations (3) and (4).

Approved for Public Release

Contrails

Martens,[2] et al, reported that the parameter H increased approximately as the square of the stress and had an Arrhenius dependence on the temperature, with activation energies in the range 90-100 kcal/mole. We found H to vary with the stress roughly as P^n, with $n \approx 1.3$ at all temperatures except 2400°C. In our activation energy plots, there was considerable scatter of the points around straight lines, particularly for the lower values of the stress. Weighting the data in favor of the higher stresses, activation energies of about 50 kcal/mole were determined. The parameter K in equation (4) was found to be either proportional to P, with considerable scatter in the data, or to vary roughly with the stress as P^n, with $n \approx 0.75$ at all temperatures except 2400°C. An activation energy for K was exceedingly difficult to determine.

The parameter β was reported by Martens,[2] et al, to be independent of the stress and temperature and to have an average value of 0.49. We also found β to be independent of the stress, in that the value of β appeared to vary at random with the stress. The same was true for the parameter γ. Table 2 gives the average values of β and γ which were determined at each temperature along with the spread in the actual values at each temperature for both parameters. Their values tended to be constant at the higher temperatures and to decrease toward the lower temperatures.

Table 2. - Average values and spread in values of exponents in power law equations (3) and (4).

Temperature °C	Average β	Range of β	Average γ	Range of γ
2300	.187	.055	.069	.035
2400	.152	.271	.066	.121
2600	.250	.131	.138	.102
2800	.356	.145	.240	.138
2900	.291	.145	.216	.108
3000	.296	.069	.224	.045

In summary, it has been found that the individual creep curves can be fitted to both equation (3) and equation (4), and fairly good fits can be obtained. With the exception of the parameter G, there is much uncertainty as to how the parameters vary with stress and temperature and as to what physical meaning the various possible relationships suggest. In the case of equation (3), there is no agreement between our results and those reported by Martens,[2] et al. Since there is disagreement not only with the results obtained using equation (3), but with other equations as well, our differences are probably due to differences in materials. However, the main objection to equations (3) and (4) is that these empirical equations offer no insight into an understanding of the phenomenon of creep in carbons.

Approved for Public Release

Contrails

3.3 Equation (2): $X = D + Et + F(1-e^{-\alpha t})$

The experimental creep curves can be fitted as well to equation (2) as to any of the other equations. But equation (2), which is now being considered, has the advantage that it can be derived from either of two fairly simple rheological models. Both models can be used to qualitatively describe the behavior of graphite in creep and in recovery after creep, and the parameters in one model are closely related to the parameters in the other model. We present both models because neither model gives a completely sufficient description of the entire behavior of the material, and there are as yet no indications as to which model may be closer to reality. The fact that there are two models which lead to the same equation means that neither model is a unique description of the material and that the parameters are open to interpretation.

A few words might be in order about the use and the value of a model. A model provides a means of simplifying and idealizing a material. The value of a model lies in its ability to provide a means of characterizing the significant features of the data both qualitatively and quantitatively in terms of simple physical ideas. If the model is a valid one, it should be able to explain and predict the behavior of the material under a variety of experimental conditions. As will be shown in this section on creep and the following section on the recovery after creep, the two models to be presented do describe very well the qualitative features of the behavior of ATJ graphite in creep and in recovery. Quantitative deviations between observed and predicted behavior serve to demonstrate the complexity of the material as opposed to the simplicity of the models, and these deviations frequently lead to ideas on how to modify the models to better describe the behavior of the material.

The two models which will be used are shown in Figure 10. Both models

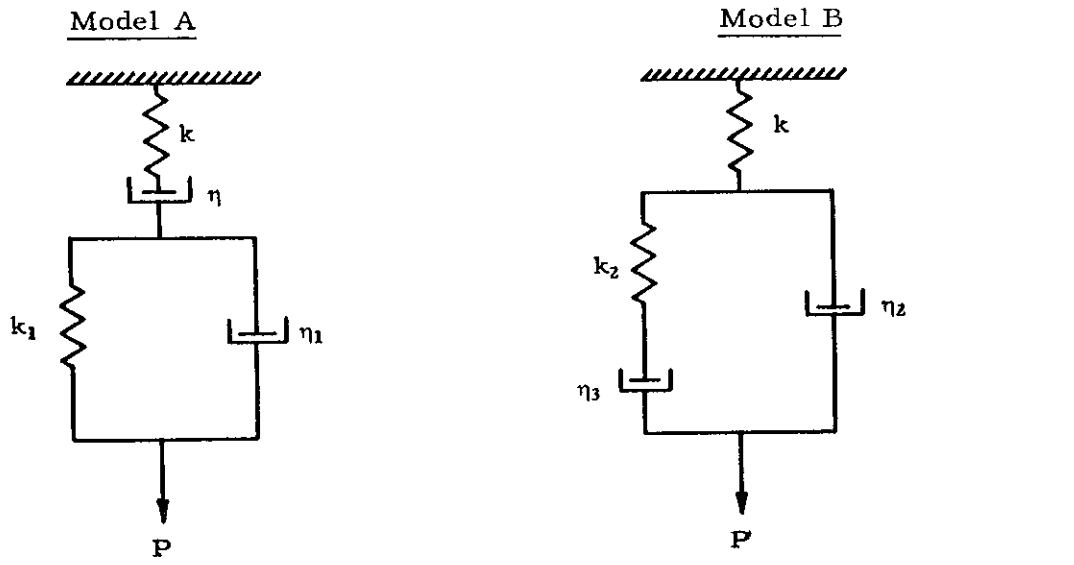

N-1119

Figure 10. - Rheological models.

Approved for Public Release

Contrails

have been well discussed in the literature to describe viscoelastic materials. Model A was first proposed by Burgers[5] and has been used by Terry[6] and by Lee and Markwick[7] to describe the behavior of pitches and asphalts. The springs represent simple elastic elements whose constants are their elastic moduli, and the dashpots represent simple viscous elements whose constants are viscosities. Under a constant load P, the deformation, as given by model A, is:

$$X = \frac{P}{k} + \frac{P}{\eta} t + \frac{P}{k_1} \left[1 - \exp\left(-\frac{k_1}{\eta_1} t\right) \right] . \qquad (2A)$$

The solution for model B under the same conditions of constant stress has been derived by Lethersich,[8] and is given by

$$X = \frac{P}{k} + \frac{Pt}{\eta_2 + \eta_3} + \frac{P}{k_2} \left(\frac{\eta_3}{\eta_2 + \eta_3} \right)^2 \left\{ 1 - \exp\left[-k_2(\eta_2 + \eta_3)t/\eta_2\eta_3 \right] \right\} \qquad (2B)$$

The main difference between equations (2A) and (2B), as far as their relationship to equation (2) is concerned, is the manner in which the parameters of the models are related to the parameters in equation (2). Model A offers a simpler appearing solution for the creep curves than does model B, though both solutions have the same general features.

The solution for model A can be qualitatively visualized in a simple manner. When the load P is applied, there is an instantaneous elastic deformation P/k due to the spring k. Under constant load, there is a constant rate of deformation P/η due to the dashpot η. The parallel combination of spring k_1 and dashpot η_1 represents an anelastic component, which leads to a time dependent rate of deformation. The maximum deformation possible from this parallel combination depends only on the spring constant k_1, and is equal to P/k_1. The time dependence for this deformation is an exponential one, the rate being determined by the ratio of the spring constant k_1 to the viscosity η_1. The solution for model B is not quite so easily visualized. The spring k again accounts for the instantaneous elastic deformation. The third term in the solution gives the so-called anelastic deformation which occurs while spring k_2 is being extended. The time dependence of the anelastic term is dependent on both η_2 and η_3, and the magnitude of this term depends on η_2 and η_3 as well as on k_2. Both dashpots η_2 and η_3 contribute to the term linear in t which dominates after spring k_2 is fully extended.

Approved for Public Release

Contrails

Equations (2A) and (2B) can be combined with equation (2) to give the following relationships between the constants in the models and the general parameters in equation (2):

Model A	Model B
$k = \frac{P}{D}$	$k = \frac{P}{D}$
$\eta = \frac{P}{E}$	$\eta_2 = \frac{P}{E+\alpha F}$
$k_1 = \frac{P}{F}$	$\eta_3 = \eta_2 \cdot \frac{\alpha F}{E}$
$\eta_1 = \frac{k_1}{\alpha} = \frac{P}{\alpha F}$	$k_2 = \frac{\alpha^2 F P}{(E+\alpha F)^2} = \frac{\alpha \eta_2 \eta_3}{\eta}$

(5)

There is fortunately a very simple one-to-one correspondence between the constants of the two models. It is found for ATJ graphite that the value of αF at any temperature is much greater than the value of E. As can be seen from inspection of equations (5), this means that k_2 is close to and slightly less than k_1, η_3 is close to and slightly less than η, and η_2 is close to and slightly less than η_1. It follows, therefore, that whatever can be said about any constant in model A follows almost exactly for its counterpart in model B.

The parameters in equation (2) were determined from the creep data in the following manner: The parameter D was read directly from the creep curve as the instantaneous deformation at zero time; D is therefore identically equal to the parameter G in equation (3). The linear part of the creep curve was then extrapolated to t = 0, and the intercept at t = 0 was taken as D + F. The parameter α was determined both from graphical analysis, by plotting log $[D+F+Et - X]$ vs t, and from the least squares program given in Appendix III. The values which were obtained from the graphical analysis are shown in Table 3.

The relationships in (5) are for model constants. In order to relate these model constants to material constants, i.e., to elastic moduli and material viscosities, the dimensions and geometry of the specimens must be taken into account. For a beam in flexure, Young's modulus M is determined from the equation

$$M = \frac{PL^3}{4Xbd^3} \quad , \tag{6}$$

where P is the force applied in flexure, b is the width of the specimen, L is the distance between supports, and X is the deformation. In a similar manner,

Approved for Public Release

Table 3. - Parameter values obtained by fitting the creep curves to equations (2), (2A), and (2B).

Temperature °C	Force Grams	(2) $X = D + Et + F(1 - e^{-at})$				MODEL A				MODEL B		
		$Dx10^4$ Inch	$Ex10^4$ In/Min	$Fx10^4$ Inch	a Min^{-1}	$kx10^{-6}$ psi	k_1x10^{-6} psi	$\eta x10^{-13}$ poise	η_1x10^{-13} poise	k_2x10^{-6} psi	η_2x10^{-13} poise	η_3x10^{-13} poise
2300	1000	72	.0313	30	.202	.837	2.00	796	4.10	2.00	4.10	796
	1500	72	.0685	42	.122	1.25	2.15	545	7.30	2.10	7.20	537
	2000	112	.167	89	.056	1.07	1.35	298	10.0	1.27	9.69	290
	2500	168	.204	80	.068	.897	1.88	305	11.5	1.74	11.1	296
2400	250	17	.021	13	.192	.885	1.16	296	2.49	1.13	2.47	294
	500	43	0	14	.116	.70	2.15	∞	7.66	2.15	7.66	∞
	1000	79	.091	46	.158	.765	1.30	274	3.43	1.27	3.39	271
	1500	86	.205	63	.183	1.05	1.43	182	3.24	1.39	3.20	179
	2000	112	.322	83	.145	1.08	1.45	155	4.15	1.38	4.05	151
	2500	188	.366	107	.180	.800	1.41	170	3.22	1.35	3.16	167
2600	250	9	.080	11	.108	1.67	1.37	77.8	3.15	.763	3.02	74.8
	500	27	.140	19	.232	1.11	1.58	89.0	2.82	1.49	2.74	86.1
	1000	85	.182	66	.055	.71	.91	137	6.80	.828	6.54	130
	1500	103	.409	124	.078	.88	.73	91.3	3.86	.670	3.71	87.7
	2000	218	.568	140	.070	.55	.86	87.6	5.09	.766	4.80	82.8
	2500	189	.926	324	.047	.795	.45	67.1	4.10	.413	3.87	63.5
2800	250	12	.100	25	.044	1.25	.602	62.3	5.65	.508	5.20	57.1
	500	44	.308	63	.046	.686	.478	40.5	4.30	.390	3.88	36.5
	1000	115	.536	123	.064	.525	.490	46.5	3.16	.427	2.96	43.5
	1500	155	1.05	260	.040	.585	.347	35.6	3.59	.290	3.28	32.5
	2000	196	1.22	480	.034	.615	.251	40.9	3.05	.218	2.85	38.1
	2500	248	3.80	601	.071	.610	.250	16.4	1.46	.210	1.34	15.1
2900	1000	99	1.02	192	.071	.610	.313	24.4	1.83	.275	1.70	22.6
	1500	170	1.50	463	.086	.531	.195	24.9	.939	.182	.905	24.0
	2000	274	3.00	647	.054	.440	.186	16.4	1.42	.158	1.31	15.3
	2500	356	4.20	904	.037	.421	.167	14.8	1.86	.131	1.66	13.2
3000	250	30	.253	41	.053	.502	.367	24.6	2.86	.294	2.58	22.2
	500	46	.492	199	.046	.657	.151	25.3	1.36	.138	1.29	24.0
	1000	123	1.01	362	.049	.490	.166	24.6	1.40	.149	1.33	23.3
	1500	202	1.98	682	.041	.547	.132	18.9	1.33	.115	1.25	17.7
	2000	304	5.53	954	.082	.397	.126	9.00	.638	.109	.595	8.40
	2500	472				.326						

Approved for Public Release

Contrails

following the example of Reiner,[5] when there is a steady rate of deformation $\dot{X}$, the viscosity can be expressed as

$$|\eta| = \frac{PL^3}{4\dot{X}bd^3} \qquad (7)$$

The model constants given in (5) were, therefore, converted into material constants by multiplying the right-hand side of every equation in (5) containing P by the factor $L^3/4bd^3$. Appropriate dimensional units were used to express the elastic constants in lb/in^2 and the viscosities in poise. The results of these calculations are presented in Table 3. In the remainder of this paper, model constants and material constants will be referred to interchangeably, but the units used in Tables and Figures will be exclusively those of material constants.

According to the models, the parameter D should be proportional to the stress. This appears to be true, as can be seen in Table 3 by an examination of the values of the spring constant k. The value of k at any temperature fluctuated at random with the stress about some average value. The only values of k which are far off the average are those obtained using the smallest loads, where the value of D was small and a small error in the measurement of D can produce a large error in k. In determining an average value of k at each temperature, the results were therefore weighted by discarding, at all but the highest temperatures, the value of k for the lowest stress. The average values of k which were determined are plotted against the temperature in Figure 11. The elastic modulus k was found to vary

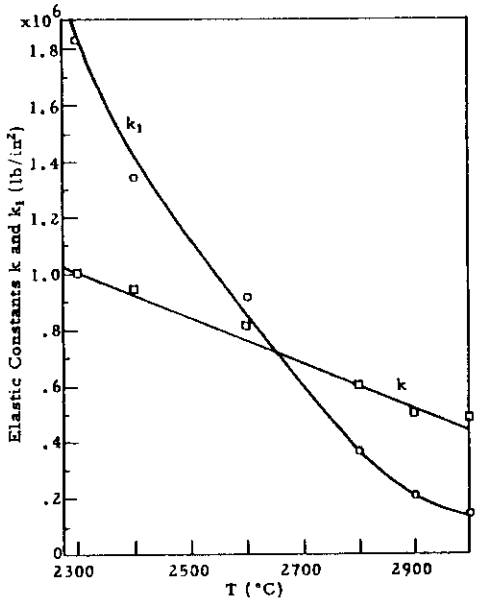

N-1036

Figure 11. - Spring constants k and k_1 as a function of temperature.

Approved for Public Release

Contrails

linearly with the temperature (in °C) according to the following relationship:

$$k = 2.84 \times 10^6 - 800T \ (lb/in^2). \qquad (8)$$

The value of the elastic modulus k, as can be seen from equation (8), is equal to 1.00×10^6 lb/in^2 at 2300°C and decreases to 0.43×10^6 lb/in^2 at 3000°C. The room temperature elastic modulus of ATJ graphite, as given in the Handbook,[9] is between 1.15 and 1.4×10^6 lb/in^2. The high temperature values of the elastic modulus which were calculated from the creep data appear to be in the correct range. One can compare our results with the curves of the dynamic modulus of ATJ graphite as measured by Lund and Bortz[10] over the temperature range from room temperature to 2500°C. Their numerical values are not in agreement either with the room temperature handbook values or with the high temperature values given here. However, they observed that the modulus increased gradually from room temperature up to about 2200°C, and then decreased with the temperature. Our results indicate that the modulus decreases linearly with the temperature between 2300°C and 3000°C.

The temperature dependence of the parameter E, the linear creep rate, can be expressed for any value of the stress as an Arrhenius function, as can be seen from Figure 12, which is a semilogarithmic plot of the creep rate E vs 1/T.

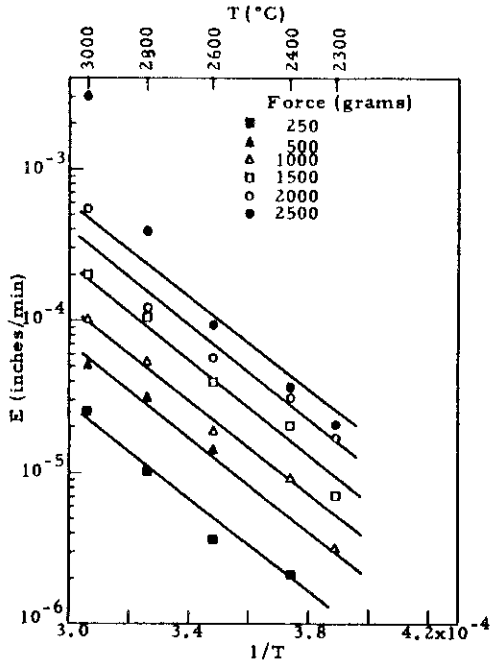

N-728

Figure 12. - Plot of steady state creep rate E vs 1/T.

Approved for Public Release

Contrails

The lines in the figure correspond to different values of the stress. From the slopes of the straight lines, an activation energy of approximately 70 kcal/mole is obtained, which appears to be the same for all values of the stress. The dependence of the parameter E on the stress itself is not so clear cut. It appears as though the creep rate may well be proportional to P for the lower stresses and then be proportional to some higher power of P as the stress is increased. In log-log plots of E vs P, it appeared that if we expressed E as being proportional to P^n, n increased with increasing load from 1 to about 1.3. Although the models contain viscosity terms which are based on conventional dashpots whose rates of flow are proportional to the load, it is quite understandable that in the creep process the rate of flow may be proportional to some higher power of the stress. We can, for example, suppose that the mechanism governing the linear creep rate is the motion of some type of defect in the material. The creep rate would then depend on the density of that type of defect and the stress. If new defects of the same type were then being generated also by the stress during the deformation, it may be that the rate of production of new defects is proportional to the creep rate while the rate of cancellation of defects is somewhat slower. With this type of mechanism, the creep rate could vary with the stress as P^n, with n somewhere between 1 and 2. The model, therefore, may have to be modified somewhat by an unconventional dashpot whose flow rate is not necessarily proportional to the first power of the stress. It can, in fact, be seen from a casual examination of the creep curves in Figures 1 to 6 that the deformation at any given time is approximately proportional to the stress at temperatures of 2300°C and 2400°C, but that it increases more rapidly as a function of stress at the higher temperatures. The creep curves themselves indicate, therefore, that at least one term in the expression for the creep must vary with some power of the stress.

By using the creep rates from the lines drawn in Figure 12, instead of the observed creep rates, it can also be shown that for the intermediate values of the stress the creep rate E is an exponential function of the applied force. By combining the temperature and force dependence of the creep rate, the creep rate can be expressed as

$$E = Q e^{-\frac{(U-cP)}{RT}} \qquad (9)$$

where U is an activation energy, Q is a constant, and c is a temperature dependent parameter. One would expect this functional dependence on the stress to break down as P approaches zero, because it would otherwise yield the unreasonable condition of a finite creep rate with zero applied force. The data indicate that equation (9) also breaks down for large values of P. The parameter c was found to increase linearly with the temperature as $c = c_1 T - c_2$. By inserting this temperature dependence of c into equation (9), we obtain

$$E = Q \exp(c_1 P/R) \exp\left[-(U + c_2 P)/RT\right] \qquad (10)$$

where $c_1 = 3.2 \times 10^{-3}$ cal/mole/gram force/°C, and $c_2 = 2.67$ cal/mole/gram force.

Approved for Public Release

Contrails

There is an apparent contradiction between equation (10), which indicates that the activation energy as determined from a plot of log E vs 1/T should increase as the stress is increased, and the results of Figure 12, which indicate that the activation energy is independent of the stress. It turns out, however, that the term c_2P in equation (10) varies, for the stresses used, from 0.67 to 6.7 kcal/mole, while the activation energy U is of the order of 70 kcal/mole. The slight changes in the slopes of the lines in Figure 12 which would be called for by equation (10) are within the limits of possible experimental error. A relationship such as equation (9) suggests that the activation energy represents a barrier which may be lowered as the external stress is increased. It indicates further that "true" activation energies may be obtained only by a careful survey of the creep rate as a function of stress.

The parameter F, according to the models, should be proportional to the stress. This parameter was more subject to experimental error than either D or E because its determination was dependent on the previous calculation of the latter two parameters. A small error in the linear creep rate E could cause a large error in the value of the intercept obtained by the extrapolation of the linear region of the creep curve back to zero time. Since the intercept gave the value of D + F, an error in one direction in D caused a corresponding error in the opposite direction in F. If F is proportional to the stress, then k_1 should be a constant independent of the stress at each temperature. Table 3 shows that there was considerable scatter at each temperature in the value of k_1. This can be due to errors in D and E and also to individual sample variations. As in the case of the spring constant k, there is no general increase or decrease in k_1 as the stress is increased, which indicates that k_1 may very well be independent of the stress. The average values of k_1 were determined, these values also being weighted by omitting the values for the specimens with the lowest applied stress as in the determination of the spring constant k. A plot of the average values of k_1 as a function of the temperature is also given in Figure 11. Since the reciprocals of the spring constants k and k_1 are direct measures of the magnitude of the elastic and anelastic components of the material, respectively (according to model A), Figure 11 indicates that the deformation is predominantly elastic at the lower temperatures and predominantly anelastic at the higher temperatures.

The parameter α, according to the models, should be independent of the stress and vary only with the temperature. The reciprocal of α has the dimensions of time and can be thought of as a relaxation time. It would be expected that as the temperature is raised, the time required to relieve the internal stresses would decrease, so that the relaxation time should decrease as the temperature is increased. In other words, α should increase as the temperature is increased. Martens,[2] et al, using a graphical method to determine α, reported that α did increase with the temperature, and that it was an Arrhenius function of the temperature having an activation energy of 148 kcal/mole. Our analysis of the ATJ data yields directly contradictory results. The value of α for ATJ graphite was found, in general, to decrease as the temperature increased. Since α is, according to model A, simply the ratio of the spring constant k_1 to the viscosity η_1, it is instructive to look at the temperature dependence of η_1. Figure 13 is a semilog plot of the average values of the viscosity η_1 vs 1/T, which shows also the spread in the actual values which were calculated at each temperature.

Approved for Public Release

Contrails

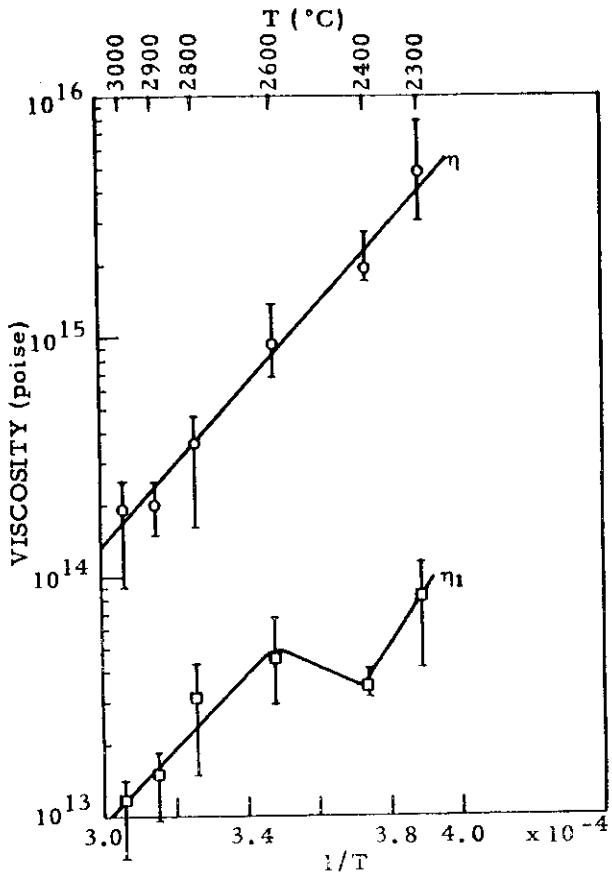

N-1037

Figure 13. - Plot of viscosities η and η_1 vs 1/T.

For comparison purposes, there is also a plot of the viscosity η vs 1/T, which can be compared with Figure 12. As in the case where average values of the spring constants were calculated, the values for the data in Table 3 corresponding to the lowest stresses were omitted in the calculation of the average values of viscosities. The points for the viscosity η fall pretty well about a straight line whose slope yields an activation energy of 76 kcal/mole, a value slightly greater than that obtained from the lines in Figure 12. The points for the viscosity η_1 do not fall simply on or about a single straight line. While the viscosity η_1 tends to decrease, in general, as the temperature increases, there is a peculiar reversal in the temperature dependence in the region between 2400°C and 2600°C. This is abnormal behavior for a single viscous element, and is an indication that the viscosity η_1 is not due to one viscous element, bu more likely to two or more anelastic components. Evidence of this is obtained from examination of the anelastic parts of the creep curves, which are obtained by subtracting from the creep curve the instantaneous elastic deformation and the linear part of the curve. The fact is that the term containing F and α in

Approved for Public Release

Contrails

equation (2), which has been called the anelastic part of the creep, is not the simple exponential function given in the equation. It is more likely that the term should be replaced by several such terms, representing parallel combinations of springs and dashpots, such as

$$\sum_i F_i (1-e^{-\alpha_i t}).$$

The actual number of such anelastic terms which are necessary will depend on the number of mechanisms which contribute to the creep. The F_i give the magnitude of the contribution from each mechanism to the anelastic part of the deformation, and the α_i provide a measure of the rate corresponding to each mechanism. Unfortunately, a creep experiment does not give sufficient information to allow us to resolve the several anelastic components. However, the conclusion that more than one anelastic component is present is supported by the analysis of the recovery curves. The problem which remains is that of resolving the different terms F_i and α_i. Some possible approaches to this problem are discussed in Section 5.

4. RECOVERY AFTER CREEP

When the load is removed after the material has undergone creep, a partial recovery of the deformation can be observed over a fairly long period of time. A typical creep and recovery curve for ATJ graphite is shown in Figure 14.

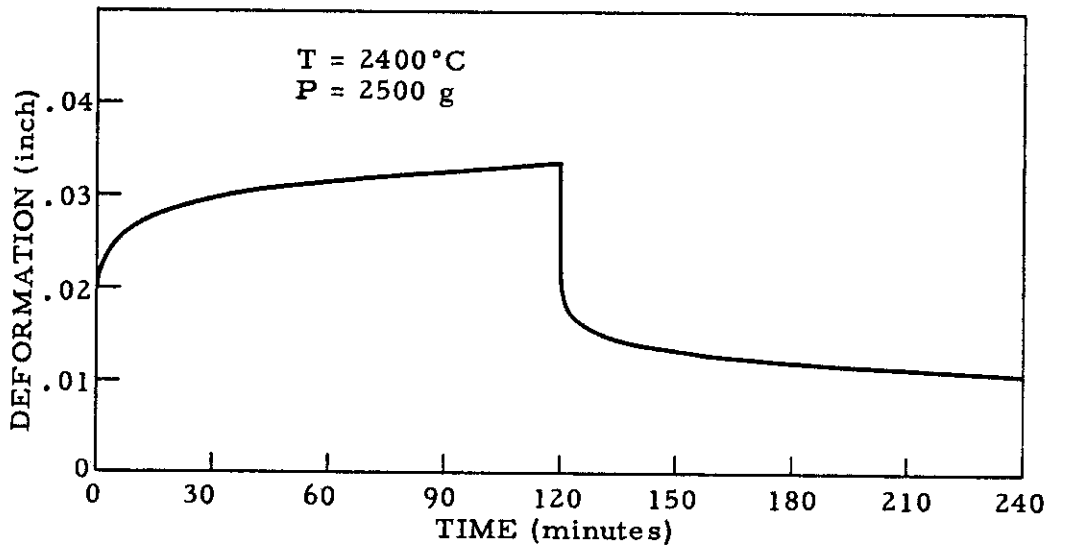

Figure 14. - Typical creep and recovery curve.

Approved for Public Release

Contrails

The specimen here was stressed at 2400°C for a period of two hours, at the end of which time the load was removed. As can be seen in Figure 14, there was an instantaneous recovery of part of the deformation, followed by a gradually decreasing rate of recovery which was not yet equal to zero at the end of two hours. In general, only a fraction of the total deformation is recoverable, and times of the order of hours are needed before the maximum possible recovery is attained. In some cases, recovery has been observed for as long as four hours without equilibrium having been attained. The behavior of graphite in creep and recovery is typical of what can be expected in a viscoelastic material.

The two rheological models shown in Figure 10 are both capable of describing qualitatively the general features of the recovery curves and can be used also to draw quantitative correlations between features of the creep and recovery curves. From the nature of the springs and dashpots, the behavior predicted by each model when the load is released after a period of creep can be visualized. During a creep test, both of the springs in each model are stretched. The spring k is stretched to the maximum extension possible for the applied load P, and the other spring to some extension equal to or less than some maximum extension which can be determined from the values of the spring constant and the load P. When the load is removed, in the case of model A, the spring k completely recovers instantaneously, and the parallel combination of spring k_1 and dashpot η_1 has a time-dependent recovery of the type given for the creep in equation (2A). In fact, equation (2A), without the term linear in t, describes the recovery completely. In the case of model B, there is also an instantaneous elastic recovery given by spring k, and there is also a time-dependent recovery as given in equation (2B) due to the combination of spring k_1 and dashpots η_2 and η_3. Because of the dashpot η in model A and the existence of two dashpots in parallel in model B, part of the deformation produced during creep is not recoverable when the load is removed.

Consideration of the models led to several tests and experiments which helped to demonstrate further the viscoelastic behavior of carbon at high temperatures, and to reveal some of the limitations of the models. The experiments which were performed can best be visualized by referring to Figure 15, which depicts what shall be called a basic creep and recovery experiment. As can be seen in Figure 15, when the load P is applied at t = 0, there is an instantaneous elastic deformation X_o, followed by a decreasing rate of creep, until some linear creep rate is attained. The time to reach some deformation X_m is τ_c. A variation in the usual creep experiment is now introduced: the specimen is allowed to be held at deformation X_m for some time τ_h. Upon removal of the load at time $\tau = \tau_c + \tau_h$, there is an instantaneous elastic recovery X_r followed by a decreasing creep rate. R represents the total amount of recovered deformation after some sufficiently long time. In order to hold the deformation at constant X_m in the experiment, a special attachment was made to fit on the apparatus to allow us to stop the lever through which the load was applied. During the hold time τ_h, a load was maintained on the specimen.

The first test of the recovery parts of the curves was a check of the values of X_r for the creep curves shown in Figures 1 through 6. Although no recovery curves are shown in the figures, the recovery was actually recorded after each of the creep tests for a period of about

Approved for Public Release

Contrails

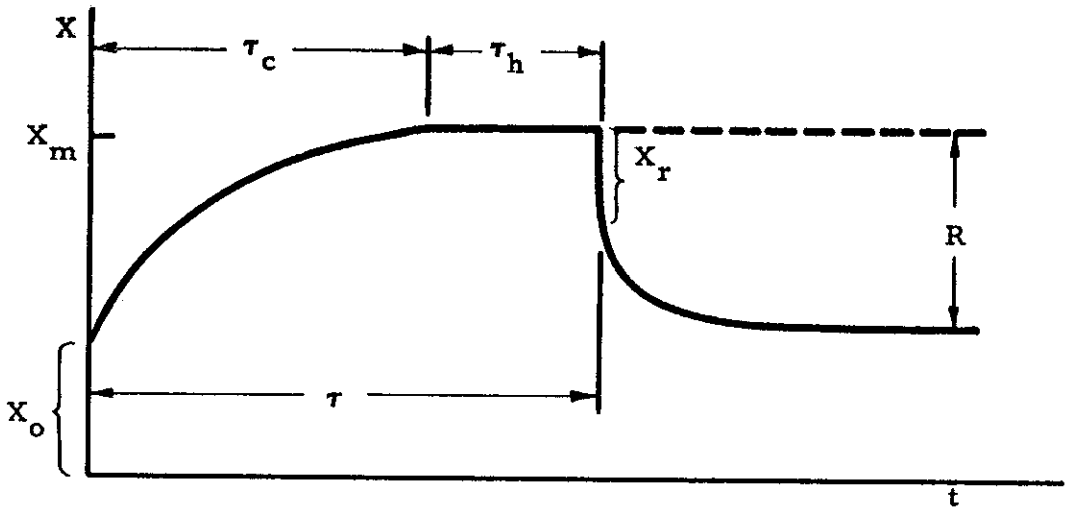

N-806

Figure 15. - Basic creep and recovery experiment.

20 minutes. According to model A, the deformation X_m, if attained after a period of time in which the creep rate is linear, should be given by

$$X_m = \frac{P}{k} + \frac{P}{\eta}\,\tau_c + \frac{P}{k_1} \quad . \tag{11}$$

When the load P is removed, the model predicts an instantaneous elastic recovery X_r given by

$$X_r = \frac{P}{k} \quad . \tag{12}$$

According to the model, the ratio of the instantaneous elastic recovery to the maximum deformation X_m should be independent of the stress, and depend only on the constants of the model and the time τ_c. By combining equations (11) and (12), the following is obtained:

$$\frac{X_r}{X_m} = \frac{1}{1 + \frac{k}{\eta}\,\tau_c + \frac{k}{k_1}} \quad . \tag{13}$$

Approved for Public Release

Contrails

Since τ_c was equal to two hours for all of the creep tests, a time long enough for a linear creep rate to have been obtained, and the time $\tau_h = 0$, the recovery data for all of the curves in Figures 1 through 6 could be used to check this relationship. Figure 16 is a plot of X_m against X_r for the specimens whose creep

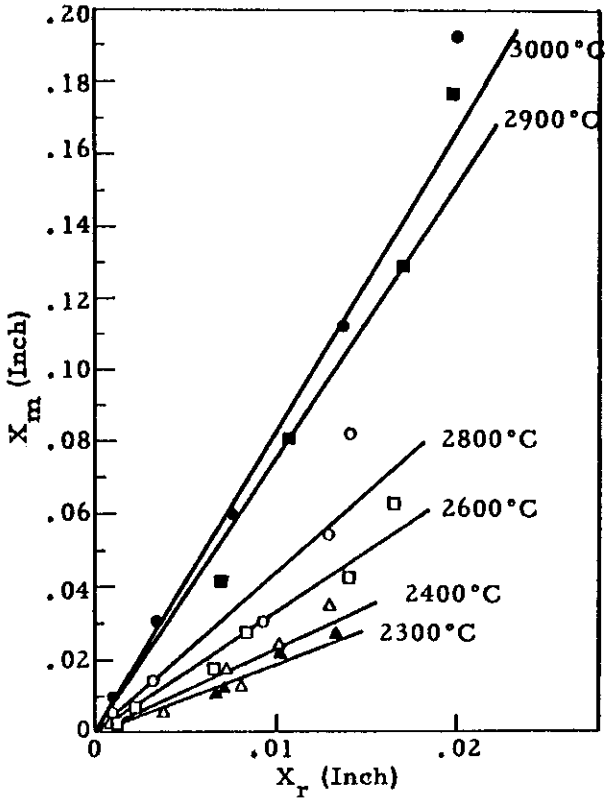

N-1121

Figure 16. - Plot of X_r vs X_m.

curves are given in Figures 1 through 6. According to equation (13), the points at any given temperature should fall on a straight line. In general, this appears to be true, though there is some scatter of the points at any particular temperature about their straight line. There appears, however, to be a systematic deviation from the straight lines toward larger values of X_m. This is not surprising. It can be recalled that the parameter E, the linear term in the creep equation, was found to have a dependence on the stress which was roughly some power of the stress slightly greater than one. This stress dependence, if introduced into the model, would cause the term $k\tau_c/\eta$ in the denominator of equation (13) to be multiplied by some fractional power of the stress, so that the ratio X_r/X_m would decrease as the stress is increased. Since the term k/k_1 is generally an order of magnitude greater than $k\tau_c/\eta$, the effect of the stress dependence of the linear creep rate on the ratio X_r/X_m is small as long as the stress is relatively small. As the stress is increased, its effect on the ratio of X_r to X_m should become

Approved for Public Release

Contrails

more pronounced. It is this decrease of the ratio X_r/X_m as X_m is increased which causes the deviations from the straight lines which can be observed in Figure 16.

Several additional experiments were performed in which the emphasis was on the recovery part of the curves. These experiments can be divided into three cases, each of which will be discussed separately. In each case, tests were made on several samples which were as identical as possible. Some of the variables shown in Figure 15 were held constant, and other of the variables were varied. The results were compared qualitatively with the predictions of the models.

4.1 Case 1

Let us consider the following experimental conditions. Let the temperature be constant, let X_m be some constant value, let $\tau_h = 0$, and vary the force P.

If we look first at the creep curves, we find that according to both models as P is increased the instantaneous elastic deformation X_o should increase and τ_c, the time to reach the deformation X_m, should decrease. Looking next at the recovery curves, the models predict that X_r and the total recovery R should both increase as the load P increases, since the extension of both springs in each model increases as P increases. Some experiments which were run at 2600°C and 3000°C demonstrated that this was the case. Figure 17 shows the results of five tests made

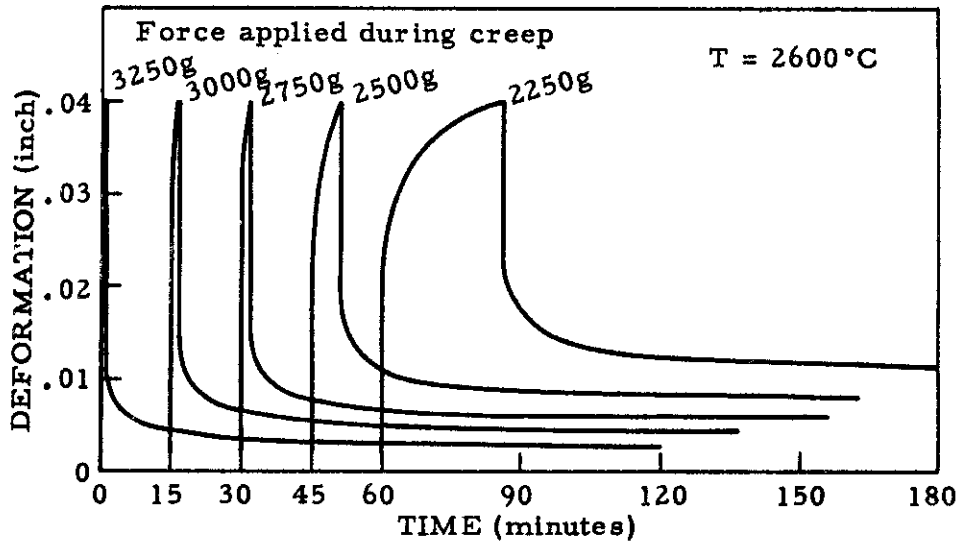

N-1122

Figure 17. - Creep and recovery at 2600°C for different applied loads.

Approved for Public Release

Contrails

at 2600°C with five different loads. The runs were plotted in Figure 17 with starting points displaced by 15-minute intervals along the time axis. Though the values of X_o cannot easily be read from the figure, the original data clearly showed X_o to increase as the load increased. It can be seen from Figure 17 that the value of X_r and R both increase as the load is increased. These results are in excellent agreement qualitatively with the predictions of the models.

4.2 Case 2

Let us consider the following conditions: Let the temperature be constant, let X_m be some constant value, let the force P be a constant (so that τ_c is also constant), and vary the hold time τ_h.

We should distinguish between two possibilities: the deformation X_m will be reached either after or before the steady state creep rate is attained. If the deformation is stopped at some value X_m after the creep rate has become constant, the conditions of the springs in the models are such that they are at the maximum possible extension for the applied load. If the deformation is suddenly held constant (and this requires the continued application of an external force), both models predict that some relaxation of the forces on the springs should occur. The forces on the springs are relieved as the dashpots flow. Notice in model A that the dashpot η continues to flow in the same direction as it flowed during the application of the external force while the dashpot η_1 flows in the opposite direction. In model B, either one or both dashpots flow in the same direction as they did during the application of the external force. The magnitude and time dependence of the displacements of the elements in model B depend in a more complicated manner than in model A on the values of the spring constants and viscosities of the elements. In both models, however, as the hold time τ_h increases, forces on both of the springs decrease, so that when the load is removed, both X_r and R should decrease.

The situation is a little more complicated if we consider the case where the deformation is stopped before the creep has reached steady state behavior. In this event, the springs k_1 and k_2 in the two models have less force on them than the spring k. If the deformation is held constant, there must first occur with time an equalization of the forces on both of the springs which takes place through the motion of the dashpots. The force on spring k will decrease with time, but the force on spring k_1 or k_2 may for a while increase and then decrease with the hold time τ_h. For the conditions stated for Case 2, where only the hold time τ_h is varied, the model predicts that both X_r and R should decrease as τ_h is increased. To test the predictions of the models, several experiments were run at 2600°C and 3000°C with different values of X_m and P, using values of τ_h varying from zero to 60 minutes. Figure 18 shows one set of recovery curves obtained at 3000°C with a load of 2000 grams, where X_m = 0.08 inch. The creep curves corresponding to the recovery curves are not shown. The deformation X_m = 0.08" was reached in times τ_c varying from 4 to 5 minutes. The variation in creep time is undoubtedly due to sample variations, and the small creep time means that steady state creep behavior had not been attained. The curves in Figure 18 are clearly in good qualitative agreement with the predictions of the models. Other groups of samples which were held at fixed deformation X_m after a steady state creep rate was reached showed the same decrease in X_r and R as the hold time τ_h was increased.

Approved for Public Release

Contrails

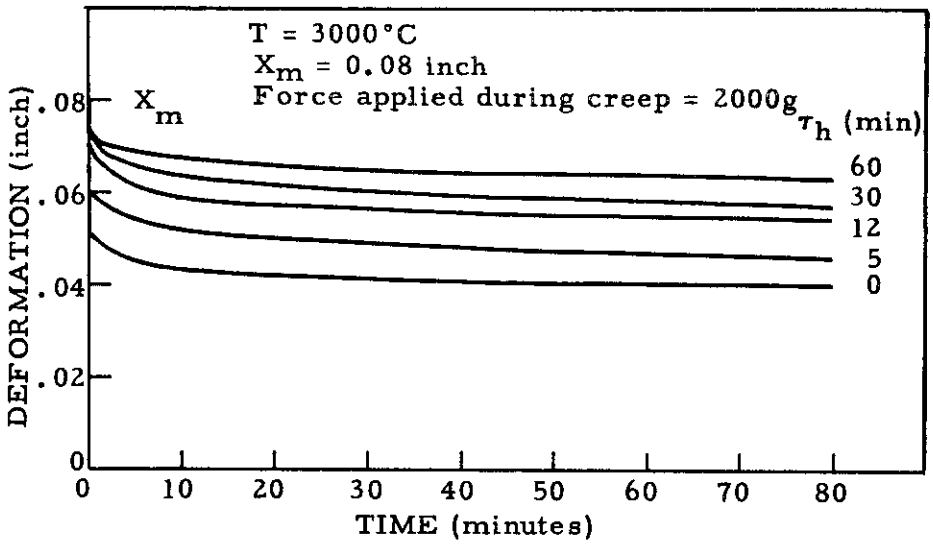

N-1039

Figure 18. - Recovery at 3000°C after different hold times.

4.3 Case 3

Let us consider the following conditions. Let the temperature be constant, let the force P be constant, let the hold time $\tau_h = 0$, and vary the creep time τ_c.

According to both models, the instantaneous elastic recovery X_r should be constant, independent of the creep time τ_c, because it should depend only on the extension of the spring k. The total amount of recovery R, however, depends on the extension of both springs in each of the models. The magnitude of R should therefore increase as τ_c increases and approach some constant value as the spring k_1 or k_2 approaches maximum extension; R should reach its asymptotic value at the same time as the creep curve enters its region of linear creep rate.

These predictions of the models were tested by running creep tests on several ATJ samples at 2600°C, with creep times varying from 15 minutes to two hours. The recovery was then observed for periods of two hours. The results are shown in Figure 19. Because of individual variations in the specimens, the creep curves for the individual specimens were not all identical. The figure demonstrates the type of variations in behavior one gets when one tries to reproduce data experimentally. On Figure 19 is a table giving the values of X_m, X_r, and R at the end of 120 minutes of recovery, as read from the original data. The value for R is really only a lower limit for the true value of R, as the recovery

Approved for Public Release

Contrails

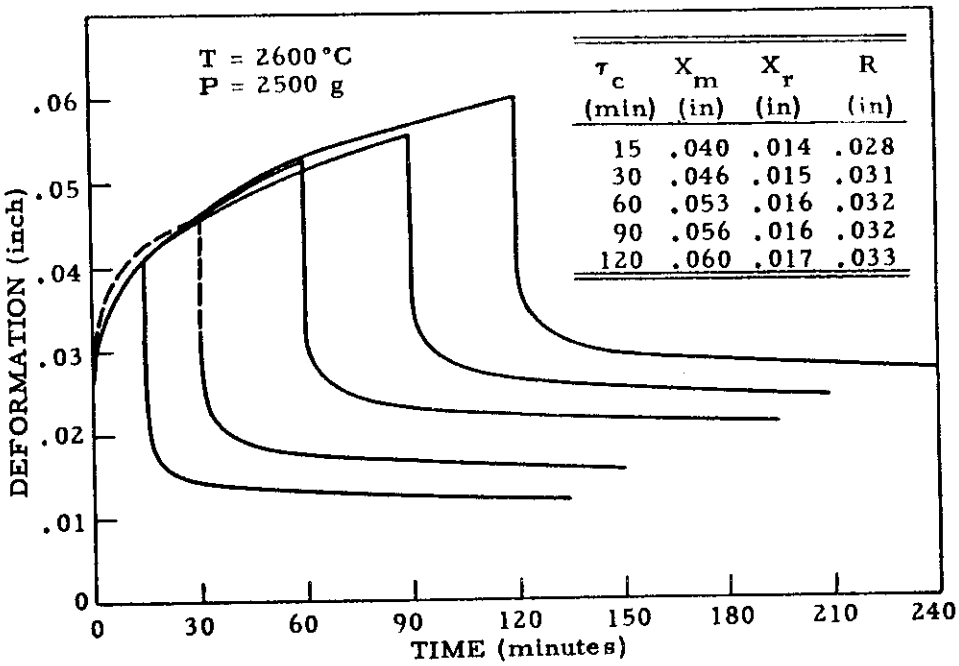

Figure 19. - Creep and recovery at 2600°C.

curves were all still decreasing at an almost linear rate at the end of two hours. The values of R tend to follow the general predictions of the model, but the values of X_r tend to increase slightly as τ_c is increased instead of remaining constant.

In each of the three cases which have been presented, the models appear to show fairly good agreement with experiment and to describe the qualitative behavior very well. There are, however, some areas of disagreement between the predictions of the model and the data in addition to those already shown which indicate that the models may have to be modified in order to more accurately describe the actual data. Some of the discrepancies between observed behavior and that predicted by the models will now be presented.

It has been found that the value of X_r, as shown in Figure 15, is always equal to or less than X_o, and the value of F as determined from the recovery curve (using equation (2) with E equal to zero) is always less than the value of F as determined from the creep curve. The reason for this may be either experimental or due to a property of the graphite. On the experimental side, one could guess that the larger value of X_o may be due either to slack in the apparatus which is taken up when the load is applied or possibly to the knife-edge biting into the material. Neither of these appear to be a valid reason, however. It has been found, in some experiments where the load has been removed and reapplied for several cycles between fixed limits, that the elastic parts of the deformation and recovery were actually equal, within the limit of experimental error. This behavior is in agreement with the models, and is taken as evidence that apparent

Approved for Public Release

Contrails

deformation due to slack in the apparatus in the absence of a load is either negligible or contributes the same amount of error to both X_o and X_r. Visual examination of the surfaces of specimens after creep in the region of the knife-edge also gives no evidence of any indentation by the knife-edge. A more likely source of error may be the assumption that all of the load is removed at the time of recovery. Since the specimen in recovery pushes against the frictional force due to the weight of the load transmission rod and also against the force of the spring in the differential transformer, there must still be an effective residual load on the specimen during recovery. This may not only cause X_r to be less than X_o, but may also account for the fact that the value of F in recovery (which depends on the spring constant k_1 or k_2) is always less than the value of F as determined from the creep part of the curve.

One difficulty in analyzing the results of a flexural experiment is that there is no simple relationship between the deformation, which is the experimentally measured variable, and the actual strains in the deformed specimen as the amount of deformation increases. The maximum strain is a function of the radius of curvature of the bent region of the specimen, and the latter decreases as the deformation increases. In order to convert deformation to strain, one must use a variable conversion factor which cannot easily be determined. The conversion of deformation to strain is fortunately quite simple in the case of simple tension. An analysis of creep data obtained in a tensile test would, therefore, be of great interest.

Another important source of disagreement between the models and the observed behavior is that the anelastic part of the recovery curve is not the simple exponential decay function given by the F term in equation (2). A similar disagreement was observed in the case of the anelastic part of the creep curves. The deviation from simple exponential behavior is even more apparent in a recovery curve. The recovery curve tends to decrease rapidly as the load is removed with a changing rate typical of a short relaxation time (or large value of α). However, there is a long period of very slow recovery which is usually observed for several hours and which is typical of a very long relaxation time (or small value of α). The shapes of the recovery curves would seem to indicate that there are two or more mechanisms having different relaxation times, which contribute to the recovery. The anelastic part of the recovery may therefore depend on a sum of anelastic components or it may be best approximated by a distribution of relaxation times. A creep experiment cannot supply sufficient information to resolve this question. However, the information obtained by means of a creep experiment may possibly be combined with information from related experiments to resolve this question of relaxation times and to give some insight into the atomic mechanisms which govern creep and recovery.

Approved for Public Release

Contrails

5. DISCUSSION

The creep and recovery experiments definitely establish the fact that graphite behaves like a viscoelastic material at high temperatures. Any attempt to describe or explain the behavior at high temperatures should, therefore, take into account the elastic, viscous, and anelastic components of the observed deformation. It is for this reason that all means of describing data by empirical equations having no physical significance are so unsatisfactory, even though it has been demonstrated that several mathematical formulas of different types can be used to give fairly good fits to the observed data. The main emphasis in the analysis of the data has, therefore, been placed on the use of mathematical forms which contain some connections with actual physical elements. We have tried to describe the behavior of graphite in creep and recovery mainly in terms of simple models.

The models which have been used are idealizations of the actual behavior, and a close comparison of the actual data with the predicted behavior of the models soon reveals areas of disagreement. It does not, however, follow that disagreement between observed data and the behavior predicted by a simple model renders the model useless or meaningless. On the contrary, the true behavior, which may not be at all simple, sometimes becomes more apparent and discernible when compared with the behavior of a relatively simple system such as is given by a model. A model may be of value in several ways. It offers primarily a means of describing both qualitatively and quantitatively in simple terms what may be a fairly complex system. This initial, fairly simple representation offers then a means of obtaining some physical insight into the actual system. In other words, a model can be used as an aid to guide one's thoughts, and it can quite often lead the experimentalist to ideas for new and varied experiments in which to test the predictions of the model. In this manner, new information arrived at by several different types of experiments can be combined into giving a single consistent picture of the actual system. During the course of an investigation, the model may have to be modified one or more times in order to consistently explain all of the observed behavior. The end result is a better model and a better understanding of the system.

Creep experiments give a limited amount of information. On the basis of the analysis of the data which has been made by using the models, one can conceive of several other types of experiments which can be performed to supply either complementary or additional information to that obtained with the creep and recovery experiments, using the models as general frames of reference. One could, for example, measure the sonic modulus of graphite over the same temperature range used in the creep experiments and compare the values of the elastic moduli thus obtained with the values of the purely elastic components which were obtained in the creep and recovery experiments. Since the relaxation times which were observed in the creep experiments were of the order of minutes or hours, the graphite should behave as a purely elastic material in a sonic modulus experiment, with an elastic modulus equal to the spring constant k in the models. Another experiment of great interest would be to determine the complex dynamic modulus for graphite by stressing the material at low frequencies, covering the

Approved for Public Release

Contrails

range of frequencies corresponding to the relaxation times which can be estimated from the creep and recovery experiments. These frequencies should lie roughly in the range from 0.01 to 10 cycles per minute. Since the analysis of the creep and recovery curves indicates that there is more than one relaxation time involved in the anelastic component of the deformation, examination of the in-phase and out-of-phase components of the dynamic modulus should either reveal resonances at definite relaxation times or indicate what type of a distribution of relaxation times can be used to describe the data. Yet another type of experiment which can be used to probe the model is a stress relaxation experiment. In this type of experiment, one would measure the force necessary to maintain a constant deformation, and one could correlate the results of this type of experiment with the recovery after partial stress relaxation. Additionally, one could also do a constant strain rate experiment, in which the stress is measured as a function of time, and relate the results of this type of experiment to the model. A good model should be capable of describing in a consistent manner the results of all of these related experiments.

The models which have been used in the analysis presented in this paper are representations which are, in our opinion, good first approximations to some ultimate true representation of the material. A final good description of creep and associated phenomena should take into account the mechanisms which contribute to the observed behavior on the atomic and microscopic scales. In the case of polycrystalline graphites, the observed macroscopic creep should depend on such factors as the density of the bulk material, the particle-binder nature of the material as determined in the fabrication process, and the size, type, and orientation of the crystallites and particles within the specimen in the particular experimental test. In our creep experiments, we concentrated on only one material and maintained the same grain orientation in the specimen in all of our tests. The model approach was encouraging, but scatter in the data due mainly to variations in the specimens made accurate determination of the parameters in the model difficult. However, if a valid model can be found for one particular type of graphite such as, for example, ATJ graphite, then it is reasonable to believe that the same model can be used for other graphites. If the data can be made more precise and reproducible, we should then be able to calculate the parameters in the model for graphites whose variable factors, as given above, are controlled. Variation of the parameters in the model with some of the above-mentioned variables in polycrystalline graphites may then lead to ideas as to which mechanisms on the atomic scale may be contributing to the observed behavior. In addition, it would be helpful if some of the parameters and the manner in which they vary with stress or temperature, could be related to the behavior of single crystals of graphite, assuming experiments on the mechanical properties of single crystals could be performed. We are still far from an understanding of the actual mechanisms which influence the high temperature mechanical properties of carbon. This paper presents an approach to the general problem of mechanical property behavior of carbon at high temperatures which may help to lead to a better characterization and understanding of the materials and their behavior.

Approved for Public Release

Contrails

6. REFERENCES

1. H. W. Davidson and H. H. W. Losty, Nature, Lond. 181, 1057-9 (1958); Mechanical Properties of Non-Metallic Brittle Materials, W. H. Walton, editor, Interscience Publishers, Inc., New York, 1958, pp. 219-38.

2. H. E. Martens, D. D. Button, D. B. Fischbach and L. D. Jaffe, Progress Report No. 30-18, Jet Propulsion Laboratory, California Institute of Technology, October 15, 1959; Proceedings of the Fourth Conference on Carbon, University of Buffalo, Pergamon Press, 1960, pp. 511-530.

3. A. H. Cottrell, Dislocations and Plastic Flow in Crystals, (The Clarendon Press, Oxford) 1953, p. 199.

4. E. N. da C. Andrade, Proc. Roy.Soc. A 84, 1 (1910); A 90, 329 (1914).

5. See M. Reiner, Deformation and Flow, H. K. Lewis and Co., Ltd., London, 1949, p. 277-280. See also Chap. XII.

6. N. B. Terry, Fuel 37, 309 (1958).

7. A. R. Lee and A. H. D. Markwick, J. Soc. Chem. Ind. (London), Trans. 56, 146T-156T (1937).

8. W. Lethersich, J. Soc. Chem. Ind. (London), Trans. 61, 101-108 (1942).

9. The Industrial Graphite Engineering Handbook, National Carbon Company, Division of Union Carbide Corporation, 1959, p. 5A.07.01.

10. H. H. Lund and S. A. Bortz, Proceedings of the Fourth Conference on Carbon, University of Buffalo, Pergamon Press, 1960, pp. 537-546.

Approved for Public Release

Contrails

APPENDIX I

FITTING OF DATA TO EQUATION (1)

The general problem in the mathematical analysis of the data was to fit a set of experimental points (y_i, z_i), where i = 1, ..., n, to a straight line of the form

$$y = a + b\,(z - \bar{z}). \tag{I-1}$$

From the method of least squares, it follows that

$$b = \frac{\sum_{i=1}^{n} z_i y_i - n\,\bar{z}\,\bar{y}}{\sum_{i=1}^{n} z_i^2 - n\,\bar{z}^2} \tag{I-2}$$

and

$$a = \bar{y}\,. \tag{I-3}$$

The bar over a letter denotes the average value of the variable over the n values of that variable. The following identities are also useful:

$$n\,\bar{z} = \Sigma\, z \text{ and } n\,\bar{z}^2 = z\,\Sigma\, z,$$

where we have dropped the subscript i under the summation sign and in the variables under the summation sign for the sake of shortening the notation.

Equation (1) of this report can be written in the form of a straight line as follows:

$$\frac{X-A}{t} = B + C\,\frac{\log t}{t}\,. \tag{I-4}$$

By analogy with equation (I-1) above, we can set $\frac{X-A}{t}$ equal to y and set $\frac{\log t}{t}$ equal to z. The parameter C can then be evaluated by means of the equation

$$C = \frac{\sum\left(\frac{X-A}{t}\right)\left(\frac{\log t}{t}\right) - \overline{\left(\frac{\log t}{t}\right)} \sum\left(\frac{X-A}{t}\right)}{\sum\left(\frac{\log t}{t}\right)^2 - \overline{\left(\frac{\log t}{t}\right)} \sum\left(\frac{\log t}{t}\right)}\,, \tag{I-5}$$

Approved for Public Release

Contrails

where the summation is over the n values of X and t which are taken from the creep data.

The parameter B can then be determined by taking the values of C as determined by equation (I-5) and using equation (I-4), averaging over the n experimental points, so that

$$B = \overline{\left(\frac{X-A}{t}\right)} - C\,\overline{\left(\frac{\log t}{t}\right)} \quad . \tag{I-6}$$

The experimental data were treated as follows: The value of A was taken directly from the creep curve as the value of X at t = 1. This is a good estimate of A because B turns out to be small compared to C. The values of $(X-A)/t$ and $\frac{\log t}{t}$ were then tabulated for equal intervals of $\frac{\log t}{t}$ ranging in steps of 0.0025 from 0.0200 to 0.0500. This corresponds to times ranging from 100 minutes to 29.3 minutes. The values of C and B were then calculated using equations (I-5) and (I-6).

Approved for Public Release

Contrails

APPENDIX II

FITTING OF DATA TO EQUATIONS (3) AND (4)

In order to use for equations (3) and (4) of the text the least squares program given in Appendix I for equation (1), the equations were rewritten in linear form. Equation (3) of the text becomes

$$\log (X-G) = \log H + \beta \log t \qquad \text{(II-1)}$$

and equation (4) of the text becomes

$$\log X = \log K + \gamma \log t. \qquad \text{(II-2)}$$

In equation (II-1) above, we can relate log (X-G) to y and log t to z. By analogy with the analysis in Appendix I, we find that

$$\beta = \frac{\sum \log t \cdot \log (X-G) - \overline{\log t} \sum \log (X-G)}{\sum (\log t)^2 - \overline{\log t} \cdot \sum \log t} \qquad \text{(II-3)}$$

and

$$\log H = \overline{\log (X-G)} - \beta \cdot \overline{\log t} \qquad \text{(II-4)}$$

The experimental data were treated in the following manner. The value of G was read directly from the data as the value of X a few seconds after the load was applied. The values of X and log t were tabulated for times ranging from 3 to 30 minutes in intervals of 3 minutes and for equal intervals of log t ranging from 1.50 to 2.00 in steps of 0.05. The latter corresponds to values of time ranging from 31.6 to 100 minutes. The values of β and H were then calculated using equations (II-3) and (II-4).

For equation (II-2) above, corresponding to equation (4) of the text, we can again use the analogy with Appendix I and relate log X to y and log t to z. We find then that

$$\gamma = \frac{\sum \log t \cdot \log X - \overline{\log t} \sum \log X}{\sum (\log t)^2 - \overline{\log t} \cdot \sum \log t} \qquad \text{(II-5)}$$

Approved for Public Release

Contrails

and

$$\log K = \overline{\log X} - \gamma \cdot \overline{\log t} \quad . \tag{II-6}$$

Values of X and t from the data were tabulated for the same values of time which were used in analyzing for equation (3) of the text. The values of γ and K were then calculated using equations (II-5) and (II-6) above. In this analysis, log t was tabulated in intervals of 0.05 from 1.5 to 2.

Approved for Public Release

Contrails

APPENDIX III

FITTING OF DATA TO EQUATION (2)

The least squares program of Appendix I given for equation (1) was applied to equation (2) of the text as follows: Equation (2) of the text was written in linear form as

$$\log [D + F + Et - X] = \log F - \alpha t \log e. \qquad \text{(III-1)}$$

The value of E was taken directly from the creep curve as the slope of the linear part of the curve where the creep rate was constant. The value of D+ F was taken as the X intercept at t = 0 of the extrapolated linear part of the curve. The values of X were tabulated over three-minute intervals for times from zero until the argument D + F + Et - X was zero. By analogy with the program in Appendix I, log [D + F+ Et - X] was related to y and t to z. It follows then that

$$-\alpha \log e = \frac{\sum t \log [D+F+Et - X] - \bar{t}\sum \log [D+F+Et -X]}{\sum t^2 - \bar{t}\sum t} \qquad \text{(III-2)}$$

and

$$\log F = \overline{\log [D+F+Et - X]} - \alpha \bar{t} \cdot \log e \ . \qquad \text{(III-3)}$$

In the actual work, equation (III-2) above was used for the determination of α, and the results were compared with the graphical analysis in which log [D + F + Et -X] was plotted against t. The graphical analysis showed that the anelastic part of the creep curve is not the single simple exponential given in equation (2) of the text, and it indicated that a better approximation to the shape of the curve might be achieved by using two or more simple exponential functions of the type given in equation (2) of the text. The value of α determined analytically using equation (III-2) above compared favorably with the best straight line fit that could be made graphically. The value of F was not determined from equation (III-3) above, but was determined from the value of D + F as obtained in the extrapolation of the linear part of the creep curve and the value of D which was read directly from the creep curve as the instantaneous deformation at t = 0.

Approved for Public Release